ORIENTAL JOURNAL OF CHEMISTRY
An International Open Access, Peer Reviewed Research Journal
www.orientjchem.org
ISSN: 0970-020 X
CODEN: OJCHEG
2025, Vol. 41, No.(3):
Pg. 831-838

Effect of Degassing Temperature on the Specific Surface Area of Some Metal Chelates

SABITHA MOHAN M. R.[1,3]. RANI PAVITHRAN*[2,3], SUNEESH C. V.[4], ATHIRA R. S.[4] and AJITH PRASAD K[5]

[1]Department of Chemistry, Central Polytechnic college, Thiruvananthapuram, Kerala, India.
*[2]Department of Chemistry, College of Engineering Trivandrum, Thiruvananthapuram, Kerala, India.
[3]Department of Chemistry, University College, Thiruvananthapuram, Kerala, India.
[4]Department of Chemistry, University of Kerala, Thiruvananthapuram, Kerala, India.
[5]Department of Chemistry, Government Arts College, Thiruvananthapuram, Kerala, India.
*Corresponding author E-mail: ranipavithran@cet.ac.in

http://dx.doi.org/10.13005/ojc/410315

(Received: August 19, 2024; Accepted: May 16, 2025)

ABSTRACT

Chelated metal coordination polymers of ADA and EDTA ligands were degassed for 12 h at different temperatures, and their specific surface area was measured by the multi-point BET method. The effect of degassing temperature on the specific surface area, pore size, and pore volume of gel-grown porous coordination polymers was investigated. PXRD, BET, SEM and FT-IR studies showed that degassing of the coordination polymers below their decomposition temperature showed significant change in the surface morphology and textural features, but it had no appreciable impact on the crystallinity of the compound. This study underscores the importance of considering degassing conditions when comparing surface area data from different sources.

Keywords: Porous coordination polymers, BET method, Degassing condition, Specific surface area, Mesoporous material, Microporous material.

INTRODUCTION

Porous materials play a vital role in science and technology. Recent advancements in synthetic methods have enabled precise control over structure and characteristics of porous materials.[1,2] Over the past decade, research has focused on regulating pore dimensions, fostering advancements beyond conventional applications in adsorption and catalysis[3-5]. The surface chemistry of these materials, particularly metal chelate-based porous coordination polymers, offers a versatile tool to address emerging environmental concerns due to their unique properties[6-9].

The commercialization of automated equipment has led to a surge in the use of the physisorption of gases as a method for determining porosity. The porous coordination polymers must be subjected to sufficient degassing for the elimination of solvent molecules for high surface areas and persistent porosity[10,11]. Even while acknowledging the

importance of degassing treatments done before gas adsorption measurements, only a very few researchers give importance to the conditions of outgassing treatments[12,13,14]. An improper activation temperature could cause the framework to collapse, or may cause an insufficient cleaning of the material surface[13,15]. The choice of temperature might be related to the thermal stability of the material under investigation, which can be obtained from corresponding TGA analysis. The effects of degassing temperature on metal chelates are, nevertheless, unreported in the literature. Thus, we have investigated the effect of temperature of the degassing process on the surface area of the metal chelates, paying particular attention to their crystallinity and morphology. In this work, the gel grown coordination polymers CaADA, SrCaEDTA and NiZnEDTA were degassed at different temperatures to discard the adsorbed gases prior to the actual surface area measurements. The crystal structure and nonlinear optical properties of CaADA, SrCaEDTA and NiZnEDTA were reported earlier[16,17,18], but this is the first report on their surface area measurements.

MATERIALS AND METHODS

The surface area and porosity of the synthesized coordination polymers CaADA, SrCaEDTA, NiZnEDTA were analysed using nitrogen adsorption-desorption experiments. Nitrogen adsorption studies were done at 77 K with a Quantachrome autosorb iQ-MP-XR gas sorption analyser and analysed using ASiQwin software. For each gas sorption test, 50 mg of coordination polymers were utilised. The samples were degassed for 12 h at various temperatures. The specific surface area was measured by the Brunauer-Emmett-Teller (BET) method[9,12,19]. The pore size was calculated by BJH technique[20,21].

RESULTS AND DISCUSSION

Surface area and porosity measurements of CaADA

In our work, we have degassed CaADA at two different temperatures. First, the compound was degassed at 150°C for a period of 12 h and its specific surface area was calculated as 8.27 m^2/g. The resulting isotherm (Fig.1) exhibits entirely reversible adsorption-desorption cycles. This shows that the interaction between N_2 and the CaADA was comparatively weak. In the isotherm of CaADA the adsorption and desorption branches coincide each other, which indicates that no adsorbed nitrogen is present in the inner small pores when the pressure is released during the desorption phase[19,22].

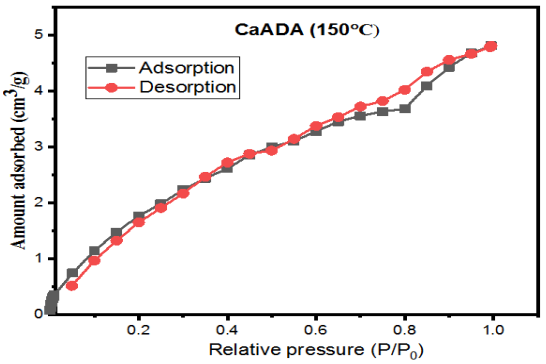

Fig. 1. Nitrogen adsorption–desorption isotherms for CaADA(150 °C at 77K

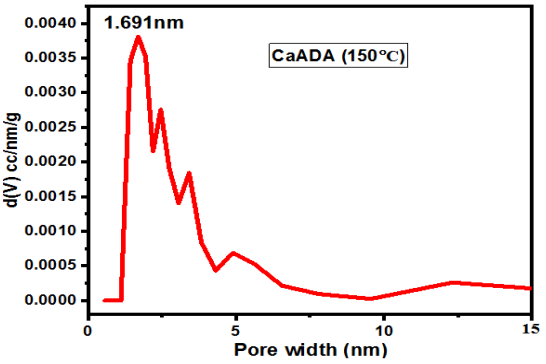

Fig. 2. BJH pore size distribution of CaADA(150°C)

The pore volume and pore diameter in CaADA were found to be 0.010 cc/g and 1.691 nm respectively. The pore distribution plot and nature of isotherm confirm that surface of coordination polymer consists of both micro and meso pores (Figure 2)[23,24].

When CaADA was degassed at 170 °C there is an enhancement in the specific surface area (13.59 m^2/g), pore volume (0.018 cc/g) and pore diameter (2.453 nm). An increase in surface area with increase in degassing temperature accounted due to the proper elimination of different impurities and moisture from the surface of the coordination polymer[10]. Here the nature of hysteresis was like Type IV[9] (Fig. 3). The pore distribution plot (Fig. 4) and nature of isotherm confirm this coordination polymer as a mesoporous material[24]. Hence it can be inferred that nitrogen adsorption capacity of CaADA can be enhanced by degassing it at 170 °C.

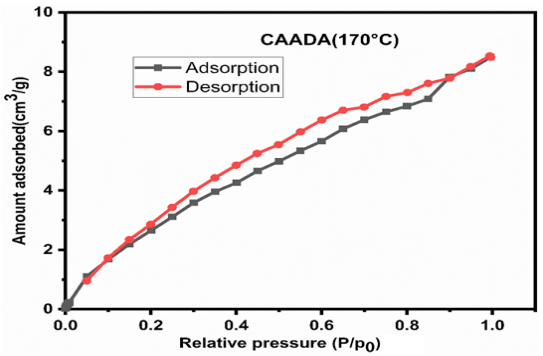

Fig. 3. Nitrogen adsorption–desorption isotherms for CaADA(170°C) at 77 K

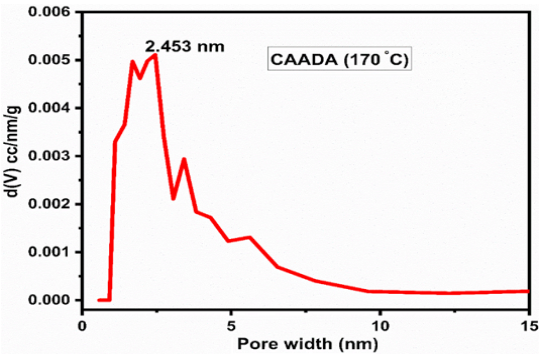

Fig. 4. BJH pore size distribution of CaADA(170°C)

Effect of degassing

Figures 5 and 6 display the IR spectra and PXRD patterns of CaADA at various degassing temperatures. It was noted that nature of bonds and the crystallinity remained unchanged during the degassing process. The PXRD patterns of the compounds following activation at various temperatures show no obvious structural changes as the degassing was conducted below disintegration temperature, obtained from the TGA of the compounds. SEM results of the formed crystals taken at various degassing conditions show that the appearance of the crystals was somewhat influenced by the activation temperature (Figure 7)

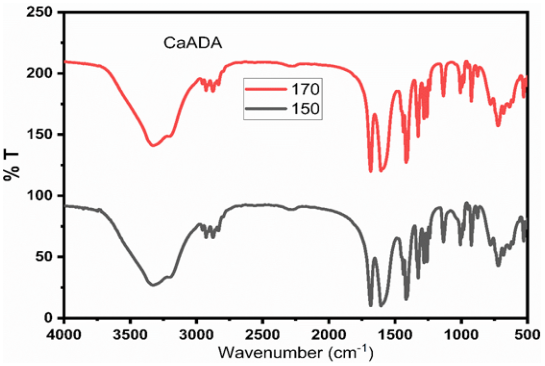

Fig. 5. FTIR spectra of CaADA (at 170°C and 150°C)

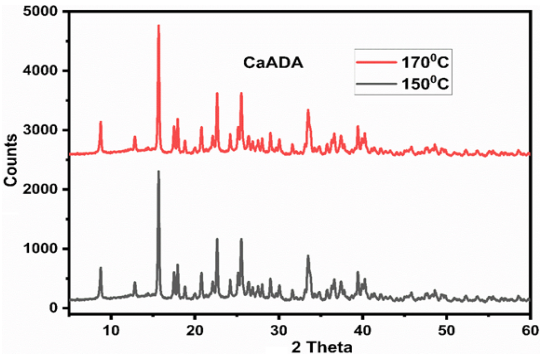

Fig. 6. PXRD patterns of CaADA (at 170°C and 150°C)

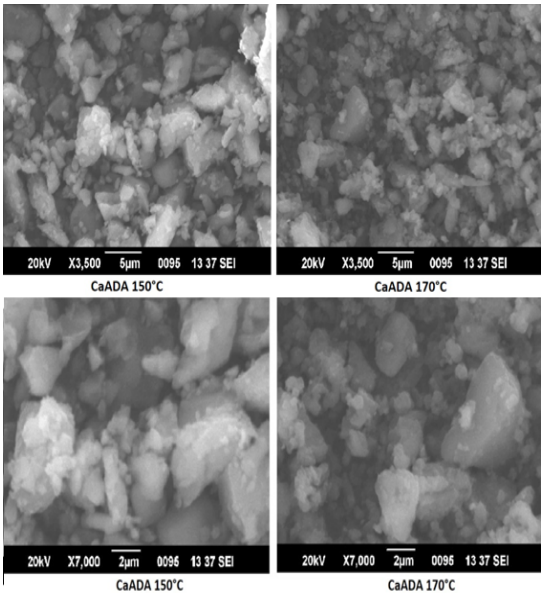

Fig. 7. SEM images of CaADA at different magnifications

Surface area and porosity measurements of SrCaEDTA

We have degassed SrCaEDTA at 80°C and 90°C temperatures before the surface area measurements. When the compound was degassed at 80°C for a period of 12 hours, the specific surface area was 8.78 m^2/g. From Fig. 8, it is evident that, like in CaADA, the interaction between N_2 and the SrCaEDTA is relatively weak at lower temperature. In the isotherm, the desorption branch coincides with the adsorption branch. This indicates that the adsorbed nitrogen does not exist in the interior narrow pores during the desorption process. Nature of adsorption-desorption graph and pore distribution diagram indicates that the coordination polymer is micro-porous in nature[25].

The pore volume and pore diameter in SrCaEDTA was found to be 0.017 cc/g and 0.686 nm respectively. Pore size distribution is shown in Figure 9.

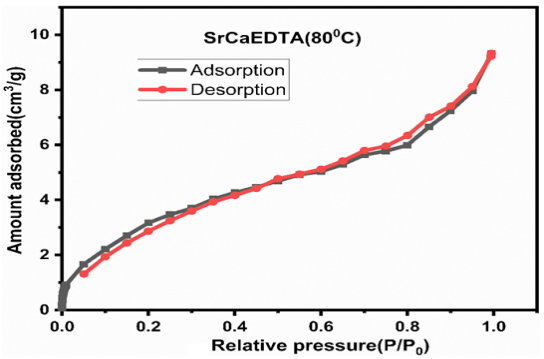

Fig. 8. Nitrogen adsorption–desorption isotherms for SrCaEDTA(80°C) at 77 K

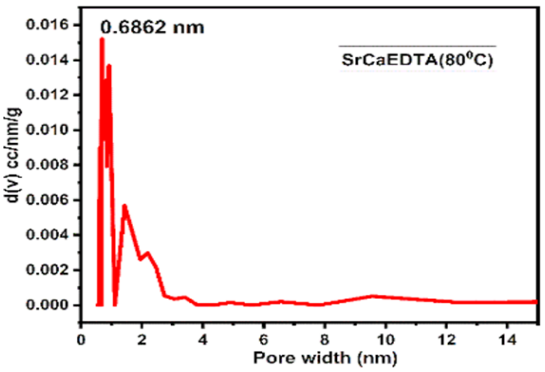

Fig. 9. BJH pore size distribution of SrCaEDTA(80°C)

When SrCaEDTA was degassed at 90°C, there is an increase in the surface area (11.953 m^2/g), pore volume (0.018 cc/g) and pore diameter (1.938 nm). Change in the degassing condition induced marked difference in surface area and pore width of SrCaEDTA. The desorption branch and the adsorption branch do not meet in the isotherm (Fig. 10). This is because the inner tiny pores of SrCaEDTA contain adsorbed nitrogen, which kinetically restricts when the pressure is released during the desorption process. The nature of the adsorption-desorption plot and pore distribution diagram (Fig. 11) show that the compound is mesoporous in nature[26].

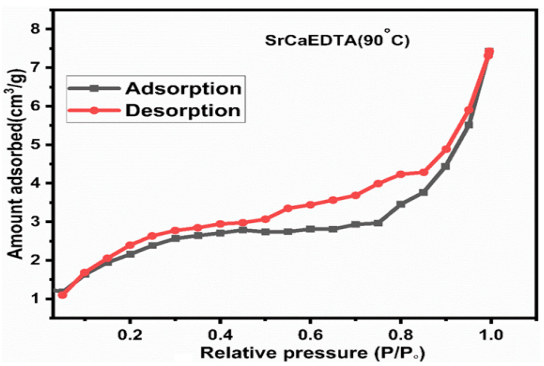

Fig. 10. Nitrogen adsorption–desorption isotherms for SrCaEDTA (90°C) at 77K

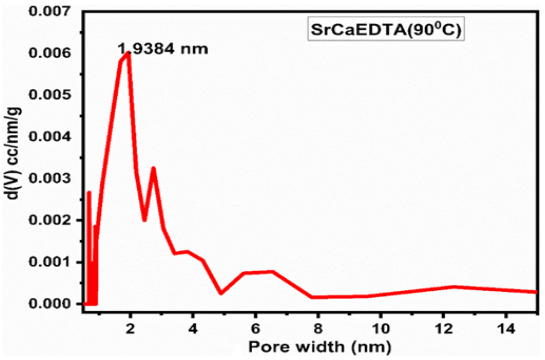

Fig. 11. BJH pore size distribution of SrCaEDTA (90°C)

Effect of degassing

Identical IR spectra and PXRD patterns are produced by gel-grown SrCaEDTA that has been degassed at 80°C and 90°C for 12 h (Fig. 12 and Fig. 13). This indicates that activation temperatures had little impact on the crystallinity of SrCaEDTA. Rather, it had a considerable impact on its surface area, porosity, and textural qualities. As no additional peaks are seen in the IR and PXRD plots, the structures of the coordination polymer will probably stay intact. However, the degassing temperature had influenced the BET surface areas along with the surface texture of SrCaEDTA (Figure 14).

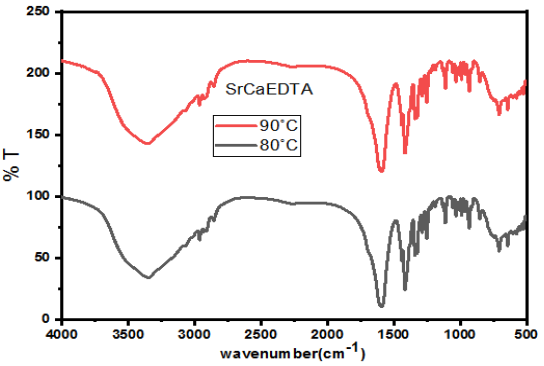

Fig. 12. FT-IR spectra of SrCaEDTA (at 90°C and 80°C)

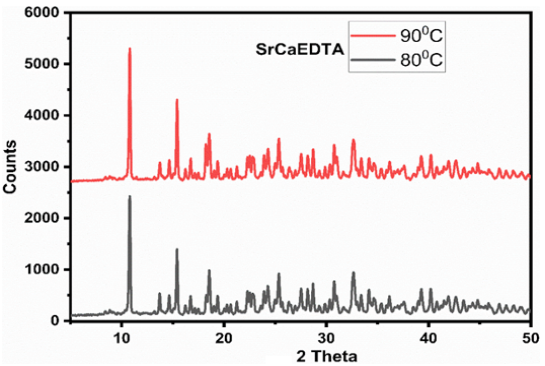

Fig. 13. PXRD patterns of SrCaEDTA (at 90°C and 80°C)

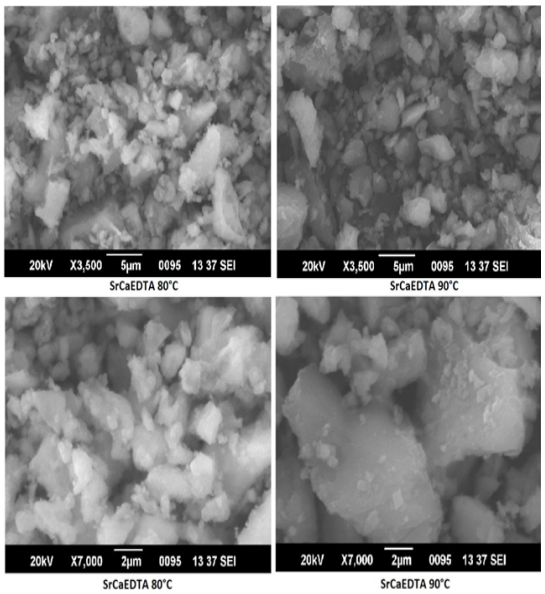

Fig. 14. SEM images of SrCaEDTA at different magnifications

Surface area and porosity measurements of NiZnEDTA

In this investigation, NiZnEDTA was degassed at two distinct temperatures. First, the substance was degassed at 80 °C for 12 hours. The specific surface area of the compound was found to be 21.876 m^2/g. The N_2 adsorption-desorption isotherms are reversible (Fig. 15). Therefore, N_2 interacts with the NiZnEDTA quite weakly and the gas was often adsorbed in the active site of the NiZnEDTA. The desorption branch coincides with the adsorption branch, indicating that adsorbed nitrogen doesn't exist in the small pores of the interior during the desorption process. The pore volume and diameter were calculated to be 2.188 nm and 0.026 cc/g in close subsequence. Fig.16 shows the pore size distribution.

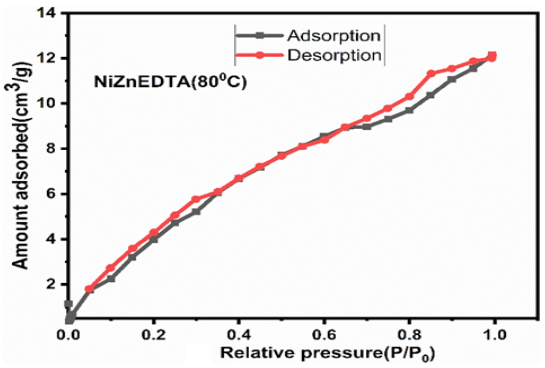

Fig. 15. Nitrogen adsorption–desorption isotherms for NiZnEDTA (80°C) at 77K

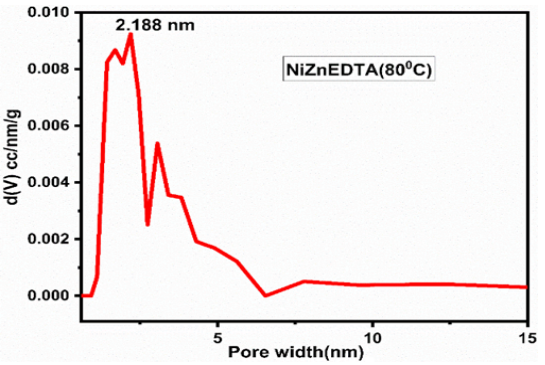

Fig. 16. BJH pore size distribution of NiZnEDTA (80 °C)

When NiZnEDTA was degassed at 90°C, an increase in surface area (25.970 m^2/g), pore volume (0,032 cc/g) and pore diameter (2.789 nm) was observed. The obtained adsorption–desorption isotherms are reversible in nature (Fig. 17). The pore distribution plot confirms the mesoporous nature (Fig. 18)[27,28]. The increase in surface area with increasing degassing temperature of the coordination polymer can be explained by the adequate elimination of moisture and other contaminants from its surface.

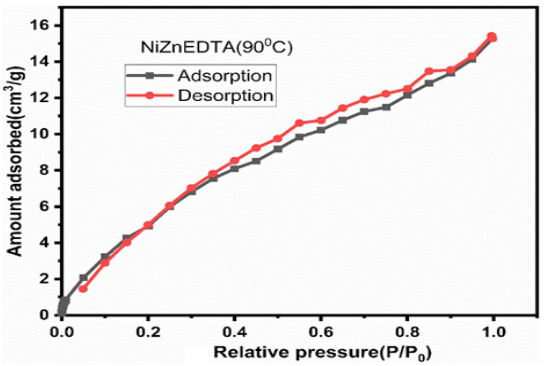

Fig. 17. Nitrogen adsorption–desorption isotherms for NiZnEDTA (90°C) at 77 K

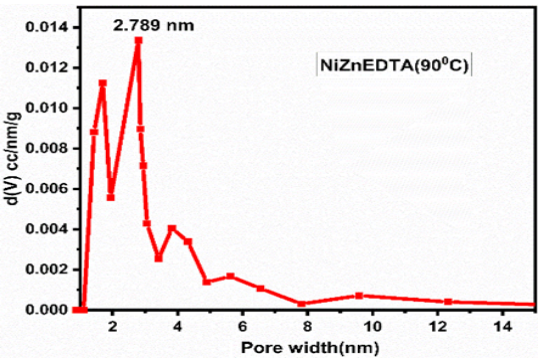

Fig. 18. BJH pore size distribution of NiZnEDTA (90°C)

Effect of degassing

NiZnEDTA, that underwent degassing at

80°C and 90°C for 12 h, failed to demonstrate any modification of the molecular structure as the IR and PXRD patterns persist unchanged (Fig. 19 and Fig. 20). The sample's surface texture altered from normal, increasing the BET surface area in the process. Thereby, it can be said that for the chosen compounds, the activation temperature only had a bearing on the surface textural characteristics (Figure 21)[10].

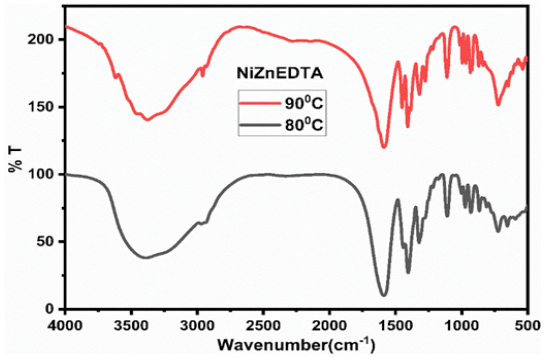

Fig. 19. FT-IR spectra of NiZnEDTA (at 90°C and 80°C)

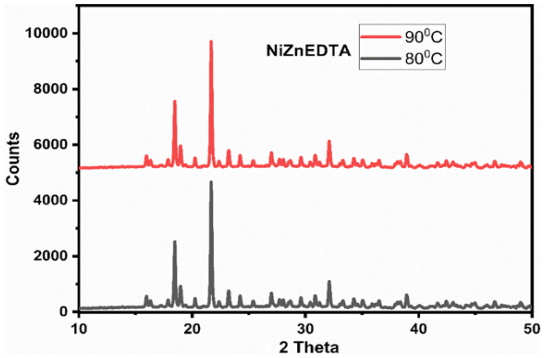

Fig. 20. PXRD patterns of NiZnEDTA (at 80°C and 90°C

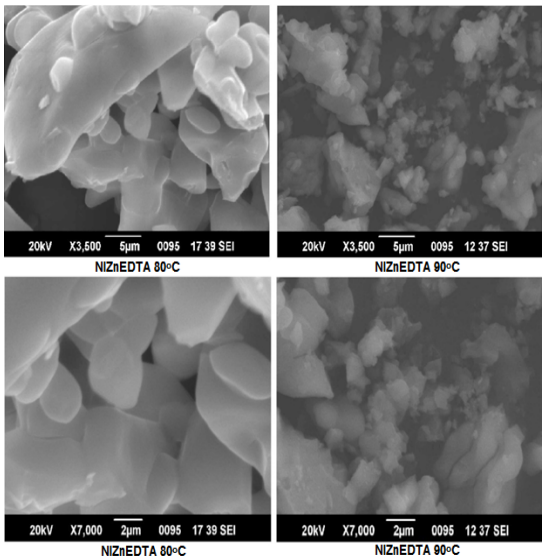

Fig. 21. SEM images of NiZnEDTA at different magnifications

Table 1 gives a comparison of surface area, pore diameter and pore volume of the three gel grown coordination polymers.

Table 1: Surface parameters of the three gel grown coordination polymers

Compound	Degassing Temperature (°C)	Surface area (m^2/g)	Pore diameter (nm)	Pore volume) (cc/g
CaADA	150	8.27	1.691	0.010
	170	13.59	2.453	0.018
SrCaEDTA	80	8.78	0.686	0.017
	90	11.953	1.938	0.018
NiZnEDTA	80	21.876	2.188	0.026
	90	25.970	2.789	0.032

The findings imply that before doing the BET surface area study, the coordination polymers have to be properly thermally degassed. We ascertained that although the crystallinity of the coordination polymers was not significantly altered by the activation temperature, the surface morphology and textural characteristics were greatly affected by deactivation.

CONCLUSION

Nitrogen adsorption studies of the coordination polymers were conducted by degassing the sample at different temperatures for 12 hours. The degassing temperature had a marked effect on the magnitude of specific surface area values of the gel grown coordination polymers. When CaADA is degassed at 150 °C and 170 °C for a period of 12 h, specific surface area enhanced from 8.27 m^2/g to 13.59 m^2/g. SrCaEDTA degassed at 80°C and 90°C for a period of 12 h, the specific surface area changed from 8.78 m^2/g to 11.953 m^2/g. Nitrogen adsorption studies of NiZnEDTA was conducted by degassing the sample at 80°C and 90°C for 12 hours. The specific surface area of the compound was found to be 21.876 m^2/g and 25.970 m^2/g respectively. The results indicate that samples should be degassed before the BET surface area analysis. Lower degassing temperature or a shorter duration of degassing, will cause incomplete cleaning of the sample surface. The degassing temperature is a crucial factor while comparing the specific surface area of a compound from different sources.

ACKNOWLEDGMENT

The authors are thankful to the authorities of Sophisticated Analytical Instrumental Facilities

(SAIF), Cochin University of Science and Technology, for providing the instrumental facilities. We also thank the Head, Department of Chemistry, University of Kerala, for providing an advanced analytical facility for BET studies.

Conflict of interest

The authors declare that they have no known competing financial interests or personal relationships that could have appeared to influence the work reported in this paper.

REFERENCES

1. Y. Liu.; L. Chen.; L. Yang.; T. Lan.; H. Wang.; C. Hu.; X. Han.; Q. Liu.; J. Chen.; Z. Feng.; X. Cui.; Q. Fang.; H. Wang.; L. Li.; Y. Li.; H. Xing.; S. Yang.; D. Zhao.; J. Li.; Porous framework materials for energy & environment relevant applications: *A systematic review, Green Energy Environ.*, **2024**, *9*, 217–310.https://doi.org/10.1016/j.gee.2022.12.010.
2. X.S. Zhao.; Novel porous materials for emerging applications., *J. Mater. Chem.*, **2006**, *16,* 623–625.https://doi.org/10.1039/b600327n.
3. B. Petrova.; B. Tsyntsarski.; T. Budinova.; N. Petrov.; C. O. Ania.; J. B. Parra.; M. Mladenov.; P. Tzvetkov.; Synthesis of nanoporous carbons from mixtures of coal tar pitch and furfural and their application as electrode materials., *Fuel Process. Technol.*, **2010**, *91,* 1710–1716.https://doi.org/10.1016/j.fuproc.2010.07.008.
4. S. Bureekaew.; S. Shimomura.; S. Kitagawa.; Chemistry and application of flexible porous coordination polymers., *Sci. Technol. Adv. Mater.*, **2008**, *9.* https://doi.org/10.1088/1468-6996/9/1/014108.
5. S. Kitagawa.; R. Kitaura.;S. I. Noro.; Functional porous coordination polymers, Angew., *Chemie-Int. Ed.,* **2004**, *43,* 2334–2375. https://doi.org/10.1002/anie.200300610.
6. M. Sánchez-Serratos.; J. R. Álvarez.; E. González-Zamora.; I. A. Ibarra.; Porous coordination polymers (Pcps): New platforms for gas storage., *J. Mex. Chem. Soc.*, **2016,** *60,* 43–57. https://doi.org/10.29356/jmcs.v60i2.72.
7. L. P. Tang.; S. Yang.; D. Liu.; C. Wang.; Y. Ge.; L. M. Tang.; R. L. Zhou.; H. Zhang.; Two-dimensional porous coordination polymers and nano-composites for electrocatalysis and electrically conductive applications., *J. Mater. Chem.* A., **2020**, *8,* 14356–14383. https://doi.org/10.1039/d0ta03356a.
8. L.H. Najim.; G.A. El-Hiti.; D. S. Ahmed.; A. Mohammed.; M. H. Alotaibi.; E. Yousif, Valsartan metal complexes as capture and reversible storage media for methane., *Appl. Petrochemical Res.*, **2020**, *10*, 77–82. https://doi.org/10.1007/s13203-020-00247-7.
9. P. Klobes.; K. Meyer.; R. G. Munro.; Porosity and Specific Surface Area Measurements for Solid Materials., *Mater. Sci.*, **2006**, *960–17*, 79.
10. C. Y. Chen.; S. C. Wu.; The effects of pretreatment on the surface properties of soils., *Chemosphere.*, **1996**, *32*, 1083–1090. https://doi.org/10.1016/0045-6535(96)00026-4.
11. D. P. Lapham.; J. L. Lapham.; Gas adsorption on commercial magnesium stearate: Effects of degassing conditions on nitrogen BET surface area and isotherm characteristics., *Int. J. Pharm.*, **2017**, *530*, 364–376. https://doi.org/10.1016/j.ijpharm.2017.08.003.
12. D. S. Phadke.; J. L. Collier.; Effect of degassing temperature on the specific surface area and other physical properties of magnesium stearate, Drug Dev., *Ind. Pharm.*, **1994**, *20,* 853–858.https://doi.org/10.3109/03639049409038335.
13. A. Figini-Albisetti, L. F. Velasco, J. B. Parra, C. O. Ania, Effect of outgassing temperature on the performance of porous materials, *Appl. Surf. Sci.*, **2010**, *256,* 5182–5186. https://doi.org/10.1016/j.apsusc.2009.12.090.
14. M. Naderi.; Surface Area: Brunauer-Emmett-Teller (BET)., *Prog. Filtr. Sep.*, **2015**, 585–608. https://doi.org/10.1016/B978-0-12-384746-1.00014-8.
15. K.O. Otun, Temperature-controlled activation and characterization of iron-based metal-organic frameworks, Inorganica Chim., *Acta.*, **2020**, *507,* 119563. https://doi.org/10.1016/j.ica.2020.119563.
16. M. R. Sabitha Mohan.; R. Pavithran.; J. I. Hubert.; T. K. Sindhu.; P. Aswathy.; Chelated calcium 1D coordination polymer: Crystal growth, characterization and Z scan studies., *J. Mol. Struct.*, **2023**, *1274,* 134474. https://doi.org/10.1016/j.molstruc.2022.134474.

17. M. R. Sabitha Mohan.; R. Pavithran.; I. Hubert Joe.; T. K. Sindhu.; P. Aswathy, Dielectric, nonlinear optical and optical limiting properties of chelated bimetallic metal-organic framework., *Opt. Mater. (Amst).*, **2023**, *138*, 113687.https://doi.org/10.1016/j.optmat.2023.113687.
18. M. R. Sabitha Mohan.; R. Pavithran.; I. Hubert Joe.; P. Aswathy, Biological, dielectric and nonlinear optical properties of chelated bimetallic 1 D coordination polymer, *Results in Chemistry*., **2024**, *11*, 101816. https://doi.org/10.1016/j.rechem.2024.101816.
19. J. Song.; wang Li.; Song Gang.; Research on influence factors on determination of specific surface area of carbon materical by N_2 adsorption method., *J. Appl. Sci. Eng. Innov.*, **2014**, *1*, 77–82.
20. Z. N. Mahmood.; M. Alias.; G. A. R. El-Hiti.; D.S. Ahmed.; E. Yousif.; Synthesis and use of new porous metal complexes containing a fusidate moiety as gas storage media., *Korean J. Chem. Eng.*, **2021**, *38*, 179–186. https://doi.org/10.1007/s11814-020-0692-1.
21. P. Klobes.; K. Meyer.; R.G. Munro.; Porosity and Specific Surface Area Measurements for Solid Materials., *Mater. Sci.*, **2006**, *79*, 960–17.http://www.ncbi.nlm.nih.gov/pubmed/22544181.
22. S. Krishnan.; C.V. Suneesh.; Post-synthetic modification of tetraphenylcyclopentadienone based hypercrosslinked microporous polymers for selective adsorption of CO_2, Mater., *Today Commun.*, **2021**, *27*. https://doi.org/10.1016/j.mtcomm.2021.102251.
23. C. G. Sonwane.; S. K. Bhatia.; Characterization of pore size distributions of mesoporous materials from adsorption isotherms., *J. Phys. Chem.* B., **2000**, *104,* 9099–9190. https://doi.org/10.1021/jp000907j.
24. L. Wu.; Y. Li.; Z. Fu.; B.L. Su.; Hierarchically structured porous materials: Synthesis strategies and applications in energy storage., *Natl. Sci. Rev.*, **2020**, *7*, 1667–1701. https://doi.org/10.1093/nsr/nwaa183.
25. D. Ongari.; P.G. Boyd.; S. Barthel.; M. Witman.; M. Haranczyk.; B. Smit.; Accurate characterization of the pore volume in microporous crystalline materials., *Langmuir.*, **2017**, *33*, 14529–14538.https://doi.org/10.1021/acs.langmuir.7b01682.
26. Z.W. Mo.; H.L. Zhou.; D. D. Zhou.; R. B. Lin.; P. Q. Liao.; C. T. He.; W. X. Zhang.; X. M. Chen.; J. P. Zhang.; Mesoporous Metal–Organic Frameworks with Exceptionally High Working Capacities for Adsorption Heat Transformation., *Adv. Mater.*, **2018**, *30*, 1–6. https://doi.org/10.1002/adma.201704350.
27. C. Liang.; J. Ren.; S. El Hankari.; J. Huo.; Aqueous Synthesis of a Mesoporous Zr-Based Coordination Polymer for Removal of Organic Dyes., *ACS Omega*., **2020**, *5,* 603–609. https://doi.org/10.1021/acsomega.9b03192.
28. C. G. Sonwane.; Suresh K. Bhatia.; Characterization of Pore Size Distribution of Mesoporous Materials from Adsorption Isotherms., *The Journal of Physical Chemistry* B., **2000**, *39*, 104. DOI:10.1021/jp000907j.